Zn^{2+} Enhances the Molecular Chaperone Function and Stability of α-Crystallin†

Ashis Biswas‡ and Kali P. Das*

Protein Chemistry Laboratory, Department of Chemistry, Bose Institute, 93/1 APC Road, Kolkata 700 009, India

Received June 18, 2007; Revised Manuscript Received November 13, 2007

ABSTRACT: α-Crystallin, the major eye lens protein, is a molecular chaperone that plays a crucial role in the suppression of protein aggregation and thus in the long-term maintenance of lens transparency. Zinc is a micronutrient of the eye, but its molecular interaction with α-crystallin has not been studied in detail. In this paper, we present results of in vitro experiments that show bivalent zinc specifically interacts with α-crystallin with a dissociation constant in the submillimolar range ($K_d \sim 0.2-0.4$ mM). We compared the effect of Zn^{2+} with those of Ca^{2+}, Cu^{2+}, Mg^{2+}, Cd^{2+}, Pb^{2+}, Ni^{2+}, Fe^{2+}, and Co^{2+} at 1 mM on the structure and chaperoning ability of α-crystallin. An insulin aggregation assay showed that among the bivalent metal ions, only 1 mM Zn^{2+} improved the chaperone function of α-crystallin by 30% compared to that in the absence of bivalent metal ions. Addition of 1 mM Zn^{2+} increased the yield of α-crystallin-assisted refolding of urea-treated LDH to its native state from 33 to 38%, but other bivalent ions had little effect. The surface hydrophobicity of α-crystallin was increased by 50% due to the binding of Zn^{2+}. In the presence of 1 mM Zn^{2+}, the stability of α-crystallin was enhanced by 36 kJ/mol, and it became more resistant to tryptic cleavage. The implications of enhanced stability and molecular chaperone activity of α-crystallin in the presence of Zn^{2+} are discussed in terms of its role in the long-term maintenance of lens transparency and cataract formation.

α-Crystallin, the major protein of the vertebrate eye lens, belongs to the small heat shock protein (sHSP)[1] family and is a molecular chaperone (*1*−*4*). It prevents the aggregation of a large number of substrate proteins, including its natural substrate β- and γ-crystallin (*5*−*10*). Under in vitro conditions, it assists the refolding of various enzyme substrates (*10*−*14*). The lens is an extremely dense mass of proteins, mainly the crystallins, with very little turnover of proteins. The chaperone function of α-crystallin is thought to be crucial in the maintenance of the transparency of the eye lens. With age, the transparency of the lens gradually diminishes and cataract develops. The causes for the gradual loss of chaperone function are not very well understood, although various post-translational modifications (*15*, *16*) and genetic mutations (*17*−*19*) are being studied in an attempt to establish any possible relationship.

Hydrophobic interaction plays a major role in the recognition of the substrate by the chaperone (*20*−*23*), and proper placement of available hydrophobic surfaces between aggregating substrate proteins is believed to be the principal mechanism for the prevention of substrate protein aggregation by the chaperones (*7*). In vitro experiments have shown that external stress conditions that exposed more hydrophobic sites were accompanied by an increase in chaperone activity (*7*, *9*). However, these conditions are nonphysiological, and how chaperone functions could be modified under in vivo conditions is still poorly understood. A recent thermodynamic study (*24*) has shown that the free energy of stabilization due to binding of a hydrophobic probe to α-crystallin does not correlate with its chaperoning ability, indicating that interactions other than the hydrophobic types may also contribute significantly to the interaction energy.

Although hydrophobic interaction in general was believed to play a dominant role in the chaperone−substrate recognition, the importance of charge interactions with respect to the polypeptide binding and structure of the chaperone was suggested by many studies (*25*−*28*). Results from our laboratory established that small anionic molecules such as ATP could significantly influence the structure, stability, and chaperone function of α-crystallin (*10*). Many recent reports indicated in vitro interaction between metal ions and α-crystallin. For example, Ca^{2+} was reported to inhibit chaperone function of α-crystallin and to promote aggregation (*29*−*31*). Cu^{2+} and Zn^{2+} were reported to induce expression of αB-crystallin in human lens epithelial cells (*32*). Cu^{2+} had been suggested to be a redox or structuring center, and Zn^{2+} was considered to act as a Lewis acid and play a structural role (*33*). Many of the crystallins such as β- and γ-crystallins are Ca^{2+} binding proteins (*34*, *35*). Several bivalent metal ions, including Ca^{2+} and Zn^{2+}, have been detected in the

† This work was supported by CSIR (India) Grants 37(1055)/00/EMR-II and 37(1218)/05/EMR-II. A.B. received a Bose Institute fellowship.

* To whom correspondence should be addressed: Department of Chemistry, Bose Institute, 93/1 APC Rd., Kolkata 700 009, India. Phone: 91 33 2303 1152. Fax: 91 33 2350 6790. E-mail: kalipada@bosemain.boseinst.ac.in or daskp25@yahoo.com.

‡ Present address: Department of Pathobiology, Cleveland Clinic Foundation, Cleveland, OH 44195.

[1] Abbreviations: sHSP, small heat shock protein; PMSF, phenylmethanesulfonyl fluoride; DTT, dithiothreitol; βME, β-mercaptoethanol; IPTG, isopropyl β-D-thiogalactoside; LDH, lactate dehydrogenase; NADH, β-nicotinamide adenine nucleotide, reduced dipotassium salt; BAPNA·HCl, *n*-benzoyl-DL-arginine-*p*-nitroanilide hydrochloride; TNS, 2-(*p*-toludino)naphthalene-6-sulfonic acid, sodium salt; bis-ANS, 4,4′-dianilino-1,1′-binaphthyl-5,5-disulfonic acid, dipotassium salt; DTNB, 5,5′-dithiobis(2-nitrobenzoic acid).

10.1021/bi7011965 CCC: $40.75
Published on Web 12/21/2007

lens, retina, and other parts of the eye (*36*−*38*). Ca^{2+} ions are believed to play a possible role in the genesis and molecular mechanism of cataract formation.

Despite these scattered works suggesting the importance of bivalent metal ions in the structural and functional properties of crystallin proteins, their mechanism of action is not understood. The published results are often contradictory to each other and do not provide much insight into the physicochemical interaction between the metal ion and α-crystallin. We have therefore undertaken a detailed study to understand the role of bivalent metal ions in the structure, stability, and chaperone function of α-crystallin. Our results clearly show that at 1 mM, of the nine bivalent metal ions chosen for this study, only Zn^{2+} has a significant effect in exposing hydrophobic groups, improving chaperone function, and enhancing the structural integrity of α-crystallin.

EXPERIMENTAL PROCEDURES

Materials. All reagents used in this study were of analytical grade. Insulin, DNase, lysozyme, *n*-benzoyl-DL-arginine-*p*-nitroanilide hydrochloride (BAPNA·HCl), isopropyl *β*-D-thiogalactopyranoside (IPTG), DTNB, calcium chloride ($CaCl_2$), magnesium chloride ($MgCl_2$), zinc sulfate ($ZnSO_4$), copper sulfate ($CuSO_4$), cobalt sulfate ($CoSO_4$), lead sulfate ($PbSO_4$), nickel sulfate ($NiSO_4$), cadmium chloride ($CdCl_2$), iron(II) chloride ($FeCl_2$), and SDS were all purchased from Sigma. *β*-Mercaptoethanol (*β*ME), dithiothreitol (DTT), trypsin, and lactate dehydrogenase (LDH) were from Sisco Research Laboratories. Tris buffer salt was purchased from GIBCO BRL. Bis-ANS and TNS were obtained from Molecular Probes. Phenylmethanesulfonyl fluoride (PMSF) was obtained from Merck.

Expression and Purification of Recombinant αA- and αB-Crystallin. Plasmids were obtained as gifts from W. W. de Jong (Catholic University of Nijmegen, the Netherlands) and J. Horwitz (Jules Stein Eye Institute, Los Angeles, CA). Methods of expression and purification of these proteins were described previously (*10*).

TNS and Bis-ANS Binding by α-Crystallin in the Presence of Different Bivalent Metal Ions. (a) TNS Binding Assay. The effect of bivalent metal ions on the exposed surface hydrophobicity of human αB-crystallin was measured with a specific hydrophobic probe, TNS. First, αB-crystallin (5.0 *μ*M) in 50 mM Tris buffer containing 100 mM NaCl (pH 7.0) was separately incubated at 25 °C for 1.0 h in the absence and presence of 1 mM different bivalent metal ions. Afterward, a methanolic solution of TNS (100 *μ*M) was added to the incubated protein samples, and the mixture was incubated for 2 h at 25 °C. The protein samples were excited at 320 nm, and fluorescence emission spectra were recorded between 350 and 520 nm. The excitation and emission band-passes were 5 nm each.

(b) Bis-ANS Binding Assay. αA- and αB-crystallin (2.5 *μ*M each) in 50 mM Tris buffer containing 100 mM NaCl (pH 7.0) were separately incubated at 25 °C for 1 h in the absence and presence of 1 mM $CaCl_2$, $ZnSO_4$, and $CuSO_4$ in a 3 mL fluorimeter cuvette placed inside a Hitachi F-4500 spectrofluorimeter maintained at the incubation temperature using a water bath. The solution was titrated with 300 *μ*M bis-ANS by adding a small aliquot at a time. After each addition, the solution was stirred magnetically for 3 min, and the fluorescence emission spectrum was recorded between 450 and 550 nm using 390 nm as the excitation wavelength. The excitation and emission band-passes were 5 nm each. To analyze the binding data according to the Scatchard equation, a titration of 0.2 *μ*M bis-ANS by 10.0 mg/mL αA- or αB-crystallin (in the absence and presence of bivalent metal ions) was performed. This reverse titration data were used to obtain the quantitative relationship between the fluorescence intensity change and bound bis-ANS, according to the work of Cardamone and Puri (*39*).

Dissociation Constant (K_d) for Binding of Cu^{2+} and Zn^{2+} to Human αA- and αB-Crystallin. Human αA- and αB-crystallin (0.05 mg/mL) were first incubated separately with 10 *μ*M bis-ANS for 2 h at 25 °C. These solutions were titrated with 10 mM Cu^{2+} or Zn^{2+} by adding a small aliquot at a time. After each addition, the solution was stirred magnetically for 1 min, and the fluorescence emission spectrum was recorded between 450 and 550 nm using 390 nm as the excitation wavelength. The excitation and emission bandpasses were 5 nm each. The equation for single-site ligand binding measured through changes in the spectroscopic signal (*40*) is given by

$$\Delta F/C_{M^{2+}} = A - K_d \Delta F \quad (1)$$

where ΔF represents the increase or decrease in fluorescence intensity at a given concentration of the bivalent metal ion, K_d is the dissociation constant, and $A = K_d \Delta F_{max}$. We used this equation to calculate the dissociation constant (K_d) for binding of Cu^{2+} and Zn^{2+} to human αA- and αB-crystallin.

Fluorescence Quenching Experiments. Tryptophan fluorescence spectra were recorded in a Hitachi F-4500 spectrofluorometer using an excitation wavelength of 295 nm. Quenching experiments were performed by separately titrating the solution of human αB-crystallin in the absence and presence of 1 mM Ca^{2+}, Cu^{2+}, or Zn^{2+} with a freshly prepared 5 M solution of acrylamide (*41*). Fluorescence intensities were measured at the wavelength corresponding to the emission maximum of αB-crystallin (337 nm) and were corrected for dilution, blanks, and inner filter effects. The effective Stern−Volmer quenching constants (K_{SV}) were calculated from the inverse slopes of the $F_0/\Delta F$ versus 1/[Q] plots according to the modified Stern−Volmer equation, $F_0/\Delta F = 1/f_a + 1/f_a K_{SV}[Q]$, where F_0 and F are the fluorescence intensities in the absence and presence of the quencher, respectively, [Q] is the molar concentration of the quencher, and $\Delta F = F_0 - F$ (*41*, *42*). The fraction of quenchable fluorescence, f_a, was obtained from the ordinate intercept of the linear portion of the $F_0/\Delta F$ versus 1/[Q] plot (*41*).

CD Measurements. Far-UV CD spectra of different samples were taken at room temperature using a Jasco J 600 spectropolarimeter continuously flushed with dry nitrogen. Spectra were collected from 250 to 200 nm using a slit width of 1 nm and a scan speed of 20 nm/min using a cylindrical quartz cell with a path length of 1 mm. Proteins (0.2 mg/mL) were dissolved separately in 50 mM borate buffer (pH 7.0) in 1 mM Ca^{2+} or 1 mM Zn^{2+} and were incubated overnight. The reported spectra were the average of five scans. Spectra were analyzed for secondary structure content by the curve fitting programs CONTINLL, CDSSTR, and SELCON3 (*43*−*45*). Near-UV CD spectra were recorded with a Jasco J-815 spectropolarimeter from 350 to 250 nm

using a 10 mm path length cell and a protein concentration of 0.5 mg/mL in the presence of 1 mM Zn^{2+} or Ca^{2+}. Appropriate control spectra were also collected and subtracted from the sample spectra.

Reactivity of Thiols in α-Crystalllin in the Presence of Bivalent Metal Ions. The free thiol concentration was measured using Ellman's reagent DTNB. First, recombinant human αA-crystallin (0.4 mg/mL) was preincubated with 1 mM Ca^{2+}, Cu^{2+}, or Zn^{2+} at room temperature (25 °C) for 1 h. Then DTNB was added to a final concentration of 0.13 mM to this mixture, and the absorbance at 412 nm was measured as a function of time with the formation of thiol nitrobenzoate anion by reaction of DTNB with the free sulfhydryl group of human αA-crystallin.

Effect of Bivalent Metal Ions on the Enzymatic Activity of Trypsin. The effect of bivalent metal ions (Ca^{2+}, Cu^{2+}, and Zn^{2+}) on the enzymatic activity of trypsin was determined using the BAPNA assay (*46*). Briefly, BAPNA [1 mg/mL in 50 mM Tris buffer containing 100 mM NaCl (pH 7.0)] was incubated with trypsin (at a ratio of 60:1, w/w) separately in the absence and presence of 1 mM $CaCl_2$, $ZnSO_4$, and $CuSO_4$ at 37 °C for 30 min. The reaction was stopped immediately by adding the appropriate amount of an acetic acid solution, and the absorbance at 410 nm was measured using a Shimadzu UV-2401PC spectrophotometer maintained at 25 °C.

Structural Stability of α-Crystallin in the Presence of Different Bivalent Metal Ions. The effect of different bivalent metal ions on the structural compactness of α-crystallin was measured by comparing the trypsin digestibility of αA- and αB-crystallin in the absence and presence of 1 mM $CaCl_2$ and $ZnSO_4$ (*10*, *23*). αA- and αB-crystallin [1 mg/mL in 50 mM Tris buffer containing 100 mM NaCl (pH 7.0)] were incubated with trypsin (at a ratio of 60:1, w/w) in the absence and presence of 1 mM $CaCl_2$ and $ZnSO_4$ at 37 °C. Aliquots were withdrawn after different periods of digestion, and the reaction was stopped immediately by adding soybean trypsin inhibitor. SDS−PAGE of the αA- and αB-crystallin digest was performed under reducing conditions in a Bio-Rad Mini-PROTEAN 3 electrophoresis setup using a linear 8 to 16% gradient polyacrylamide gel. Silver staining was used to detect the bands. Gels were scanned in a densitometer for quantitative analysis.

The effect of different bivalent metal ions (Ca^{2+}, Cu^{2+}, and Zn^{2+}, 1 mM each) on the stability of αA- and αB-crystallin was also determined by equilibrium chemical denaturation experiments (*10*, *47*). The α-crystallin solution [0.1 mg/mL in 50 mM Tris buffer containing 100 mM NaCl (pH 7.0)] was incubated at 25 °C at various urea concentrations in the range of 0−8 M for 18 h. Tryptophan fluorescence spectra of all solutions were taken in the 300−400 nm region using 295 nm as the excitation wavelength and 5 nm each for excitation and emission band-passes. The equilibrium unfolding profile was fitted according to a three-state model (*10*, *47*, *48*).

Chaperone Activity Assays of α-Crystallin in the Presence of Different Bivalent Metal Ions. The chaperone-like activity of recombinant human αB-crystallin in the absence and presence of 1 mM $CaCl_2$, $MgCl_2$, $CoSO_4$, $PbSO_4$, $NiSO_4$, $CdCl_2$, $FeCl_2$, $CuSO_4$, and $ZnSO_4$ was studied using βME-induced aggregation of insulin (*23*, *31*, *49*). Briefly, 0.32 mg/mL insulin in 50 mM Tris buffer and 100 mM NaCl (pH 7.0) in the absence and presence of 0.08 mg/mL αB-crystallin was separately preincubated with all nine bivalent metal ions at 1 mM and 25 °C for 1 h. Aggregation was initiated by adding freshly prepared βME to a final concentration of 25 mM, and the apparent absorbance at 400 nm was monitored in the kinetic mode using a Shimadzu UV-2401PC spectrophotometer maintained at 25 °C. Assays were also conducted using recombinant αA-crystallin using a 1:0.4 (w/w) insulin:αA-crystallin ratio.

Chaperone activity was also assayed by assessing the α-crystallin-mediated refolding of LDH, a homotetrameric enzyme, from its fully unfolded state (*10*). LDH was denatured in 8 M urea for 8 h at 25 °C at a concentration of 1 μM. Refolding of the enzyme was initiated by diluting the denatured LDH 100-fold in a refolding buffer (pH 7.0) comprising 50 mM Tris buffer, 100 mM NaCl, 10 mM magnesium acetate, 10 mM βME, 30 μM αB-crystallin, and/or 1 mM $CaCl_2$, $CuSO_4$, $NiSO_4$, $FeCl_2$, or $ZnSO_4$. Control experiments without αB-crystallin and/or 1 mM $CaCl_2$, $CuSO_4$, $NiSO_4$, $FeCl_2$, or $ZnSO_4$ were also conducted. The enzyme concentration was 10 nM during refolding. The activity of the refolded enzyme was assayed by adding 20 μL of refolding mixture to 580 μL of refolding buffer mentioned above containing 0.1 mM NADH and 0.4 mM sodium pyruvate preincubated at 37 °C and measuring the decrease in absorbance at 340 nm with time.

Statistical Analysis. All the values are represented as means ± the standard deviation ($n = 3$). We used Student's *t*-test to analyze the statistical differences between groups. *P* values of ≤ 0.05 were considered statistically significant.

RESULTS

Effect of Bivalent Metal Ions on the Chaperone Function of α-Crystallin. Bivalent metal ions have been reported to affect the chaperone activity of α-crystallin (*29*−*31*). Since the reports are inconsistent, we carried out an extensive chaperone activity assay of recombinant human αA- and αB-crystallin using an insulin aggregation assay in the presence and absence of 1 mM Ca^{2+}, Mg^{2+}, Pb^{2+}, Co^{2+}, Ni^{2+}, Cd^{2+}, Cu^{2+}, Fe^{2+}, and Zn^{2+} ions to probe for a specific ion effect. The results for the chaperone activity of αA- and αB-crystallin are presented in panels A and B of Figure 1, respectively. For these experiments, a ratio of 1:0.4 (w/w) of insulin to αA-crystallin or 1:0.25 (w/w) of insulin to αB-crystallin was chosen to produce ∼50% protection in aggregation in the absence of added bivalent metal ions. It should also be mentioned here that the reaction mixture contained 100 mM NaCl which maintained the ionic strength of the medium. Changing NaCl to KCl or CsCl produced no difference for any of the assays mentioned above (data not shown), indicating that the monovalent ions had no influence on the chaperone activity of α-crystallin and the changes were due to the different bivalent cations. Percentages of protection under the experimental condition calculated from the scattering value at 3 h are shown in Figure 1C. Figure 1A shows that 1 mM Ca^{2+}, Mg^{2+}, Pb^{2+}, Cd^{2+}, and Co^{2+} did not influence the insulin aggregation much. Ni^{2+} and Fe^{2+} reduced chaperone activity of αA-crystallin, but Cu^{2+} slightly enhanced it. For αB-crystallin (Figure 1B), chaperone activity was least affected by Ca^{2+}, Mg^{2+}, and Pb^{2+}, decreased by Co^{2+}, Fe^{2+}, Ni^{2+}, and Cd^{2+}, and slightly

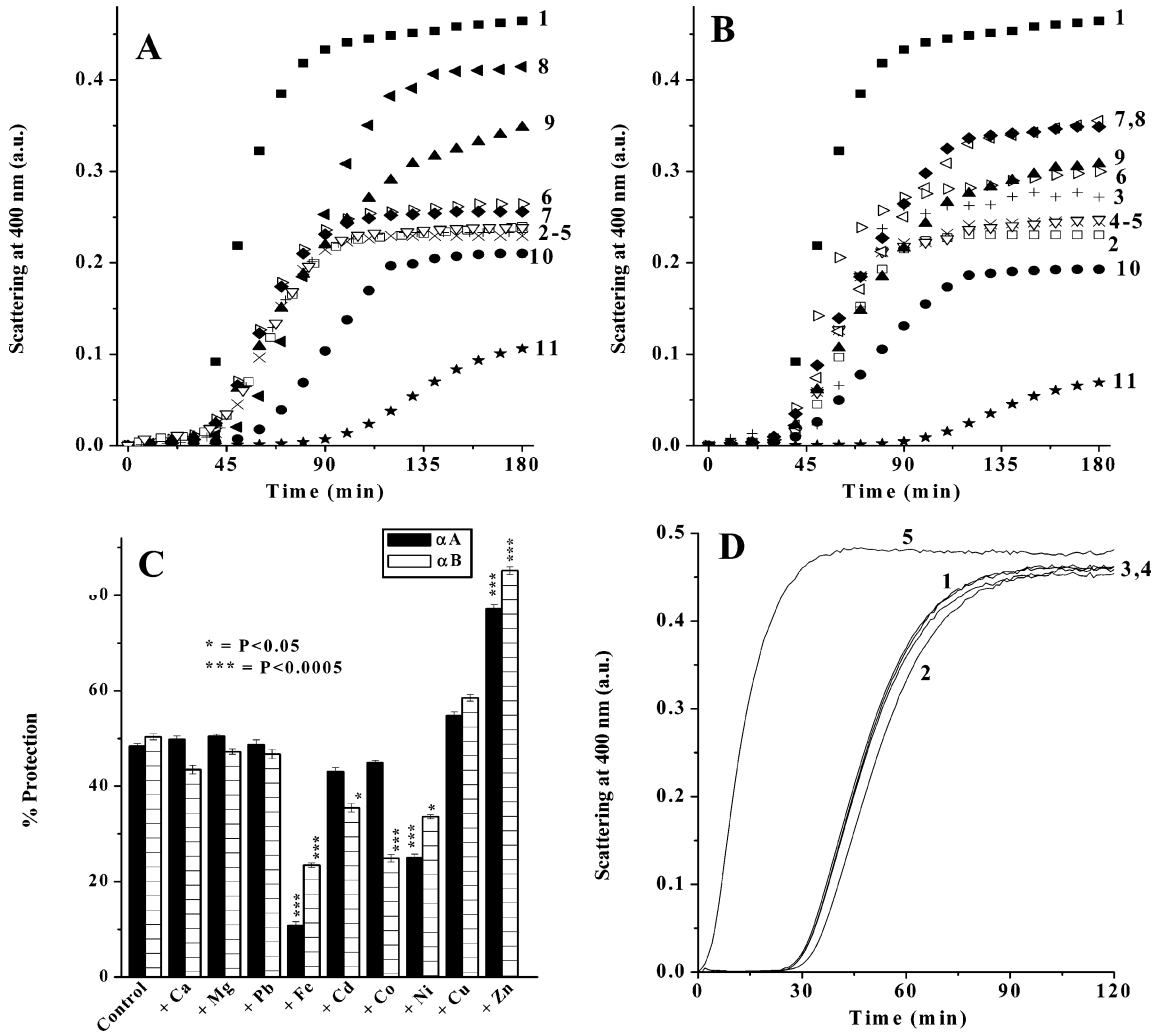

FIGURE 1: Effect of 1 mM bivalent metal ions on the chaperone activity of α-crystallin. (A) Chaperone activity of αA-crystallin and (B) chaperone activity of αB-crystallin: (1) insulin only, (2) insulin and α-crystallin, (3) insulin, α-crystallin, and Ca, (4) insulin, α-crystallin, and Mg, (5) insulin, α-crystallin, and Pb, (6) insulin, α-crystallin, and Cd, (7) insulin, α-crystallin, and Co, (8) insulin, α-crystallin, and Fe, (9) insulin, α-crystallin, and Ni, (10) insulin, α-crystallin, and Cu, and (11) insulin, α-crystallin, and Zn. The assay mixture (600 μL) contained 50 mM Tris buffer (pH 7), 100 mM NaCl, 0.32 mg/mL insulin, 1 mM bivalent metal ions, and 0.128 mg/mL αA-crystallin or 0.08 mg/mL αB-crystallin, and aggregation was started by adding 25 mM βME. (C) Percent protection ability of αA- and αB-crystallin against insulin aggregation in the absence and presence of different bivalent metal ions. Data are means ± the standard deviation from triplicate determinations. Statistically significant changes are shown with asterisks atop the bar. (D) Effect of 1 mM bivalent metal ions on the control βME-induced aggregation of 0.32 mg/mL insulin in the absence of αB-crystallin at 25 °C: (1) insulin, (2) insulin and Fe, (3) insulin and Ni, (4) insulin and Cu, and (5) insulin and Zn.

increased by Cu^{2+}. Some of these results are contrary to published results (*29*, *30*), but we have verified our results by repeated experiments with both recombinant and α_L-crystallin. Considering a 5% error in the measurement of protection, the enhancement of chaperone activity by Cu^{2+} can be considered marginal. However, the presence of 1 mM Zn^{2+} resulted in significantly ($P < 0.0005$) enhanced protection against aggregation for both αA- and αB-crystallin. In the presence of 1 mM Zn^{2+}, the chaperone function of αA- and αB-crystallin increased by ∼27 and 35%, respectively (Figure 1C). We also carefully checked if the metal ions had any influence on the control insulin aggregation assay. We found that except for Zn^{2+}, none of these metal ions at a concentration of 1 mM has any significant influence on the aggregation of insulin in the absence of αA- or αB-crystallin (Figure 1D). In the presence of 1.0 mM Zn^{2+}, the process of aggregation of control insulin (in the absence of αA- or αB-crystallin) became quicker as the lag time was significantly reduced and consequently saturation in insulin aggregation was reached early compared to that in the absence of Zn^{2+}. However, the extent of aggregation (scattering) in the presence and absence of Zn^{2+} remained practically unchanged.

The protection ability of αA- and αB-crystallin toward βME-induced insulin aggregation was found to be dependent on Zn^{2+} concentration (Figure 2). In the presence of 0.1 mM Zn^{2+}, the protection abilities of αA- and αB-crystallin were ∼59 and ∼68%, respectively, and these increased to ∼77 and ∼85%, respectively, at 1.0 mM Zn^{2+} (Figure 2B−D). It has been found that while complete prevention of aggregation required a 1:0.75 (w/w) ratio of insulin to αB-crystallin in the absence of any bivalent ion, in the presence of 1 mM Zn^{2+}, a ratio of 1:0.4 (w/w) of insulin to αB-crystallin was sufficient to give full protection (data not shown). Interestingly, the extent of maximum insulin aggregation in the absence of α-crystallin was found to be almost independent of the concentration of Zn^{2+} ions (Figure 2A). The insulin aggregation profiles in the presence of 0.1−

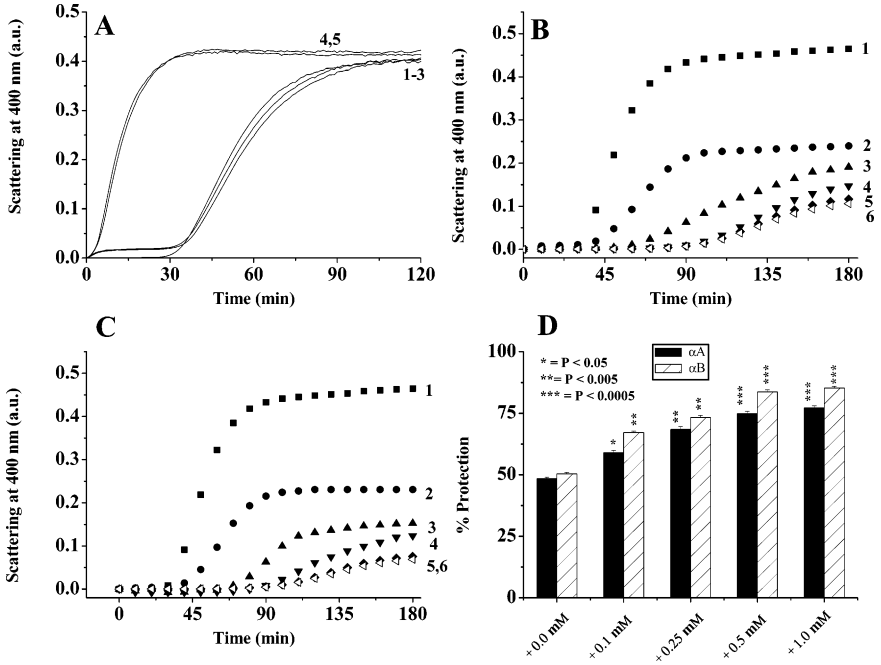

FIGURE 2: Effect of different zinc concentrations on the chaperone activity of α**A-** and αB-crystallin. (A**)** βME-induced aggregation of 0.32 mg/mL insulin in the absence and presence of 0.1−1.0 mM Zn^{2+} at 25 °C: (1) insulin, (2) insulin and 0.1 mM Zn, (3) insulin and 0.25 mM Zn, (4) insulin and 0.50 mM Zn, and (5) insulin and 1.0 mM Zn. Insulin (0.32 mg/mL) was incubated separately with or without 0.1−1.0 mM Zn^{2+} for 1 h at 25 °C. Aggregation was started by adding 25 mM βME, and scattering at 400 nm was monitored. (B) Effect of Zn^{2+} concentration on chaperone activity of αA-crystallin and (C) effect of Zn^{2+} concentration on chaperone activity of αB-crystallin: (1) insulin, (2) insulin and α-crystallin, (3) insulin, α-crystallin, and 0.1 mM Zn, (4) insulin, α-crystallin, and 0.25 mM Zn, (5) insulin, α-crystallin, and 0.5 mM Zn, and (6) insulin, α-crystallin, and 1 mM Zn. αA- or αB-crystallin was incubated separately with or without 0.1−1.0 mM Zn^{2+} for 1 h. The substrate:αA-crystallin and substrate:αB-crystallin ratios (w/w) were 1:0.4 and 1:0.25, respectively. All solutions contained 25 mM βME. (D) Percent protection ability of αA- and αB-crystallin against insulin aggregation in the absence and presence of 0.1−1.0 mM Zn^{2+} at 25 °C. Data are means ± the standard deviation from triplicate determinations. Statistically significant changes are shown with asterisks atop the bar.

0.25 mM Zn^{2+} were quite similar to that in the absence of Zn^{2+} (Figure 2A). The profile at 0.5 mM Zn^{2+} was identical with that at 1.0 mM Zn^{2+}, showing quicker aggregation but aggregation to the same extent as in the absence of Zn^{2+} (Figure 2A). Similar results were also obtained when bovine α_L-crystallin was used instead of recombinant αA- or αB-crystallins (data not shown). These data clearly show that the dose-dependent chaperone activity is primarily due to interaction between Zn^{2+} and α-crystallin.

α-Crystallin is also known to assist the in vitro refolding of many enzyme substrates (*10*−*14*). We studied the refolding of lactate dehydrogenase (LDH) at 37 °C by recombinant αB-crystallin in the presence and absence of 1 mM Ca^{2+}, Cu^{2+}, Ni^{2+}, Fe^{2+}, and Zn^{2+} ions by 100-fold dilution of an 8 M urea solution of LDH into refolding buffer (Figure 3). In the absence of both αB-crystallin and bivalent metal ions, only 4% activity could be recovered. This value did not change much in the presence of 1 mM bivalent ions in the absence of the αB-crystallin (data not shown). In the presence of αB-crystallin without any bivalent metal ions, ∼33% activity could be regained. Separately, when αB-crystallin and 1 mM Ca^{2+} or Cu^{2+} were present, the reactivation yield remained 33−36%. Furthermore, in the presence of Fe^{2+} or Ni^{2+}, the reactivation yield slightly decreased to 28−30%, but when the refolding buffer contained both αB-crystallin and 1 mM Zn^{2+}, activity recovered jumped to 48%. This effect of Zn^{2+}, leading to a significant ($P < 0.05$) increase in refolding yield, was observed when αB-crystallin was replaced with αA- and α_L-crystallin and also with other substrates such as malate dehydrogenase or carbonic anhy-

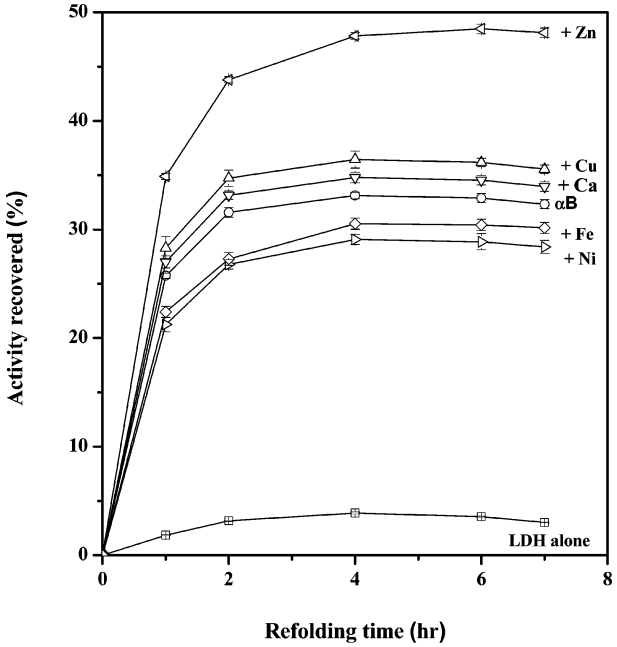

FIGURE 3: Time course of reactivation of LDH at 37 °C from an 8 M urea solution in the presence and absence of different bivalent metal ions at 1 mM. LDH was inactivated by incubation at 25 °C in an 8 M urea solution at 8 h. Refolding was initiated by 100-fold dilution of LDH (1 μM) in 8 M urea in a refolding buffer [50 mM Tris containing 100 mM NaCl (pH 7.0)] containing 10 mM magnesium acetate, 10 mM βME, 30 μM αB-crystallin, and/or different bivalent metal ions at 1 mM. Each data point is the average of triplicate measurement, and error bars denote the standard deviation.

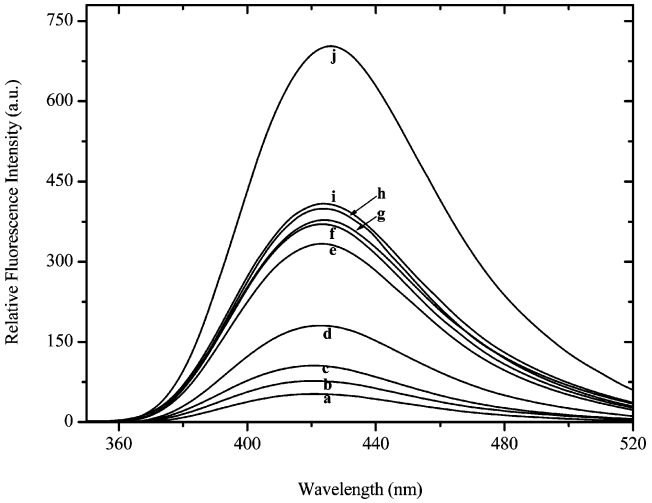

FIGURE 4: Fluorescence spectra of TNS bound to αB-crystallin in the absence and presence of 1 mM bivalent metal ions at 25 °C. The protein concentration was 0.1 mg/mL and the TNS concentration 100 μM. All protein solutions were first incubated with different bivalent metal ions at 1 mM for 1 h and then incubated with TNS for 2 h. The fluorescence spectrum of different samples was taken from 350 to 520 nm. The excitation wavelength was 320 nm: (a) Cu, (b) Fe, (c) Co, (d) Ni, (e) Mg, (f) no bivalent metal ion, (g) Ca, (h) Cd, (i) Pb, and (j) Zn.

drase (data not shown). Thus, both the insulin aggregation and the refolding activity assay revealed marked enhancement of chaperone activity of α-crystallin in the presence of Zn^{2+}.

Change in the Surface Hydrophobicity of α-Crystallin Due to Zn^{2+} Binding. Hydrophobic exposure has been probed by the fluorescence of TNS bound to αB-crystallin in the presence and absence of the bivalent metal ions. Figure 4 shows the fluorescence spectrum of 100 μM TNS separately incubated with 5 μM αB-crystallin containing 1 mM bivalent metal ion. When the intensity values at 420 nm (around λ_{max}) were compared, we found that the presence of 1 mM Zn^{2+} led to a near doubling of the fluorescence intensity. No significant changes were observed in the presence of Pb^{2+}, Cd^{2+}, Ca^{2+}, and Mg^{2+}. On the other hand, Ni^{2+}, Co^{2+}, Fe^{2+}, and Cu^{2+} led to a significant decrease ($P < 0.005$) in fluorescence intensity. This effect was not due to ionic strength because the effect was observed in the presence of 100 mM NaCl, which was sufficient to screen all electrostatic interactions.

The effect was quantitatively studied for selected bivalent ions by using bis-ANS as the hydrophobic probe (Figure 5). The result showed that the presence of 1 mM Zn^{2+} enhanced the bis-ANS fluorescence ~2.5-fold, but the same concentration of Ca^{2+} had very little effect (Figure 5A). Bis-ANS fluorescence decreased significantly ($P < 0.005$) in the presence of Cu^{2+} ion. All these results are qualitatively similar to those presented in Figure 4. To further characterize the binding of bis-ANS to αB-crystallin in the presence of the bivalent metal ions in terms of binding constant and number of binding sites, αB-crystallin was fluorimetrically titrated by bis-ANS in the presence and absence of 1 mM Ca^{2+}, Cu^{2+}, and Zn^{2+}. The fluorescence emission intensities of bis-ANS in the presence of αB-crystallin at 500 nm as a function of bis-ANS concentration are shown in Figure 5B. The data were analyzed according to the Scatchard equation (eq 2). A reverse titration of bis-ANS with recombinant αB-crystallin in the presence of the respective bivalent metal ion was necessary to convert the fluorescence intensity changes into bound bis-ANS as discussed previously (*10*, *39*).

$$\tilde{\nu} = n - K_d \frac{\tilde{\nu}}{S} \quad (2)$$

where $\tilde{\nu}$ is the number of moles of bis-ANS bound per mole of αB-crystallin, n is the number of binding sites, and K_d is the dissociation constant. Values of dissociation constant K_d and the stoichiometry of binding (n) of bis-ANS per mole of αB-crystallin subunit obtained from the Scatchard plot are presented in Table 1. It can be seen that the presence of 1 mM Zn^{2+} increased n for binding of bis-ANS to αB-crystallin from 0.97 to 2.24 per subunit and decreased K_d from 1.78 to 1.08 μM, but the presence of Ca^{2+} ion has little effect on the increase in the number of exposed hydrophobic sites of αB-crystallin (Table 1). A very similar type of result was found for αA-crystallin also (data not shown).

The bis-ANS fluorescence enhancement by Zn^{2+} and quenching by Cu^{2+} were not specific to αB-crystallin only as αA-crystallin also had a similar effect (Figure 6). In Figure 6A, we present the results for the fluorescence titration of a bis-ANS−αA-crystallin complex by Zn^{2+} and Cu^{2+}. The data for both metal ions display typical curvature, which is an indication of the "static effect" in fluorescence quenching or enhancement. Such an effect arises due to the binding of the ions to the fluorophore (*42*, *50*) which in this case is the bis-ANS−αA-crystallin complex. The data were analyzed according to eq 1, and the dissociation constant (K_d) was obtained from the slope of the linear plot of $\Delta F/C_{M^{2+}}$ against ΔF (Figure 6B). The dissociation constants (K_d) for the binding of Zn^{2+} to αA- and αB-crystallin are 0.38 and 0.20 mM, respectively, and those for binding of Cu^{2+} are 0.38 and 0.26 mM, respectively. The values are consistent with stronger interaction of these ions with αB-crystallin than with αA-crystallin. These K_d values are 1 order of magnitude lower than those obtained for the binding between bivalent metal ions and GroEL (*28*), indicating more specific interaction of these ions with α-crystallin. Since little change in fluorescence intensity was observed in the presence of Ca^{2+}, it was not possible to calculate the dissociation constant for this ion by this method.

EDTA is an effective chelator of bivalent cations. Addition of EDTA to the Zn^{2+}-containing bis-ANS and αB-crystallin solution gave interesting results. At a bis-ANS concentration of 10 μM, 0.05 mg/mL αB-crystallin in the absence of any bivalent metal ion had a fluorescence intensity of 1330 (arbitrary units) at 500 nm (Figure 7). In the presence of 1 mM Zn^{2+}, the value increased to 2700. Addition of 1, 2, 4, and 8 mM EDTA resulted in intensity values of 2550, 2780, 2850, and 3020, respectively. This indicates that the effect of Zn^{2+} ions on the surface hydrophobic exposure of αB-crystallin is not reversible. Although the Zn^{2+} ion-induced surface hydrophobic exposure was somewhat reduced at 1 mM EDTA, a higher concentration of it exposed additional sites. When 2 mM EDTA was added to a bis-ANS/αB-crystallin mixture without bivalent metal ions, the intensity at 500 nm rose from 1330 to 1750. This clearly reflects the fact that the interaction of the negative charges of EDTA on the chaperone surface can also modulate the surface hydro-

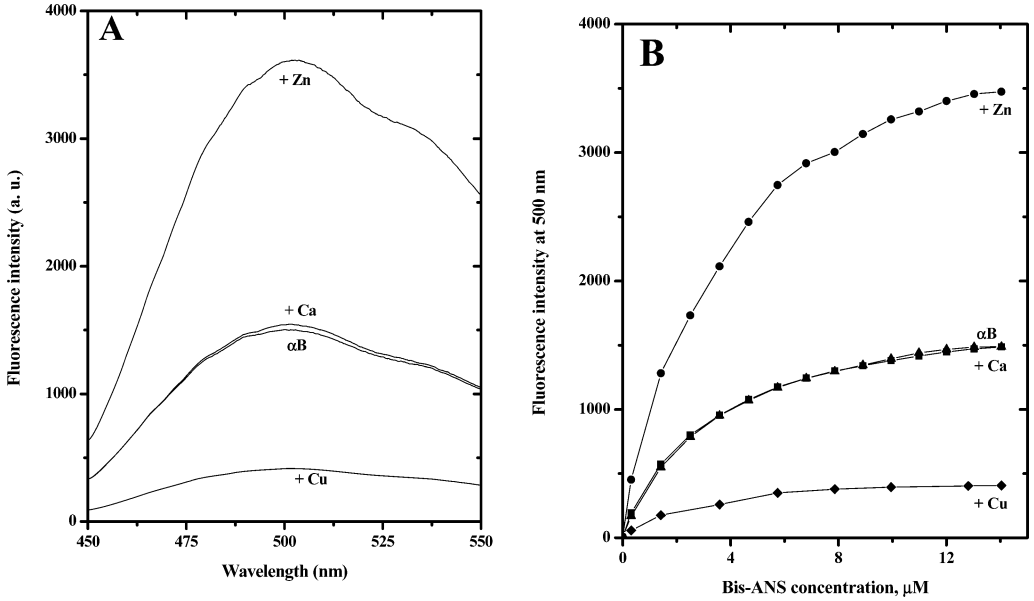

FIGURE 5: Fluorescence properties of bis-ANS bound to αB-crystallin in the absence and presence of bivalent metal ions at 25 °C. (A) Fluorescence spectra of bis-ANS in the absence and presence of 1 mM bivalent metal ions. The protein concentration was 0.05 mg/mL, and the bis-ANS concentration was 10 μM. The fluorescence spectrum of different samples was taken from 450 to 550 nm. The excitation wavelength was 390 nm. (B) Binding of bis-ANS to αB-crystallin in the absence and presence of 1 mM bivalent metal ions at 25 °C. The protein concentration in all samples was 0.05 mg/mL in 50 mM Tris buffer containing 100 mM NaCl (pH 7.0). An excitation wavelength of 390 nm and an emission wavelength of 500 nm were used.

Table 1: Parameters of Binding of Bis-ANS to αB-Crystallin in the Presence and Absence of Various Bivalent Metal Ions at 25 °C

system	n	K_d (μM)
human αB	0.97 ± 0.010	1.78 ± 0.033
human αB and 1 mM Ca^{2+}	0.99 ± 0.014	1.76 ± 0.028
human αB and 1 mM Zn^{2+}	2.24 ± 0.016	1.08 ± 0.024

phobic exposure, very much like that of ATP (*10*). Since the presence of both EDTA and Zn^{2+} does not replace the effect of each but shows a positive effect of exposing more hydrophobic groups than when present individually, it indicates that Zn^{2+} and EDTA bind to αB-crystallin at different sites.

Internal Changes in the Structure of α-Crystallin in the Presence of Bivalent Metal Ions. The results described above clearly show that the bivalent metal ions, Zn^{2+} in particular, increased the surface exposure of the hydrophobic groups. Whether these surface changes were accompanied by changes in the polarity of the buried tryptophan group has been checked by assessing the tryptophan fluorescence quenching of αB-crystallin by acrylamide in the presence and absence of the bivalent metal ions. The quenching data were analyzed by a modified Stern−Volmer equation (*41*, *42*), which enabled us to calculate the quenching constant (K_{sv}) and the fraction of accessible fluorophore (f_a) (Table 2). It is clear from Table 2 that the quenching parameters in the presence and absence of bivalent metal ions are nearly identical, indicating that the buried tryptophan environment remained unaffected.

We also probed the secondary and tertiary structure of αB-crystallin in the presence and absence of Ca^{2+} and Zn^{2+} by far- and near-UV circular dichroism (Figure 8). Most of the experiments described in this paper were carried out in 50 mM Tris buffer. However, due strong absorbance below 210 nm, the Tris buffer was replaced with borate buffer (50 mM). In the presence and absence of Ca^{2+} and Zn^{2+} ions, there were no significant changes in the CD spectrum of the protein (Figure 8A), indicating minimal changes in the secondary structure. All the spectra reflect characteristics of dominant β-sheet structure. The spectra were quantitatively analyzed with CONTINLL (*43*), SELCON3, and CDSSTR (*44*, *45*). We estimated ~32% β-sheet and 15% α-helix content which agree well with secondary structural estimates for αB-crystallin in the absence of bivalent metal ions (*51*−*53*). Therefore, at 1 mM, neither Zn^{2+} nor Ca^{2+} ions perturbed the secondary structure to any detectable extent.

Near-UV CD spectra are shown in Figure 8B. It was found that in the presence and absence of 1 mM Ca^{2+}, the near-UV CD spectral characteristics of αB-crystallin remained nearly unchanged. In the presence of 1 mM Zn^{2+} also, the spectrum exhibited almost all the features present in the absence of bivalent metal ions, although a general increase in the ellipticity value was noticed. However, no significant development of positive ellipticity was observed in the presence of Zn^{2+}. These results indicate that tertiary contacts around the aromatic residues remain largely unaltered. These results are consistent with our tryptophan fluorescence quenching data.

Reactivity of αA-Crystallin Thiols in the Presence of Bivalent Metal Ions. αA-Crystallin has two free thiol groups located at the junction of the "α-crystallin" domain and the C-terminal tail at positions 131 and 142, respectively (*2*). It is already known that of these two thiols, the one at position 131 was accessible to thiol-reacting reagents while the one at position 142 was buried (*54*). Thiol residues can coordinate to bivalent metal ions through their available electron pair on the sulfur atom, and this would result in a lack of thiol reactivity. We determined the accessibility of the thiol groups toward the reagent DTNB at room temperature in the presence of the bivalent metal ions by following the time course of the product absorbance at 412 nm (Figure 9). In the absence of any bivalent metal ion, A_{412} rose sharply for

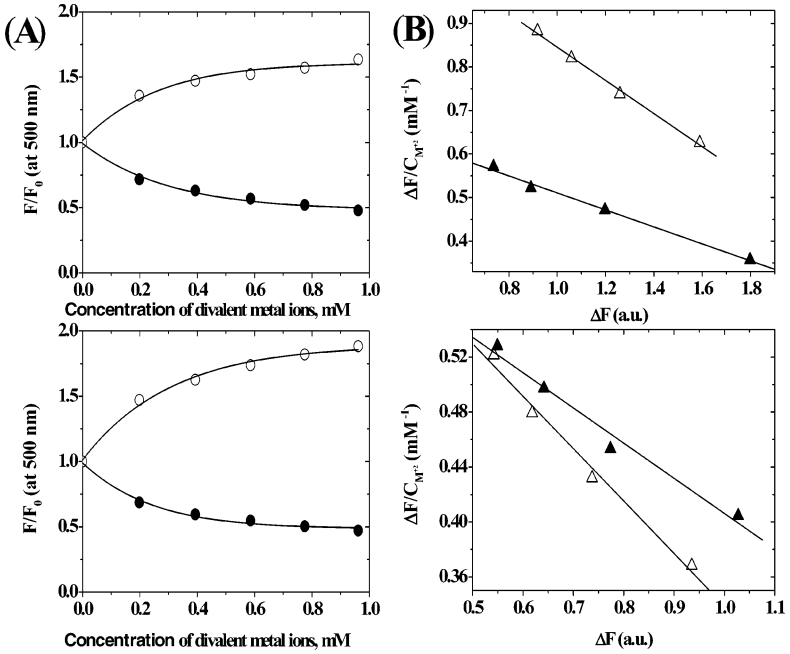

FIGURE 6: Binding of Cu^{2+} and Zn^{2+} ions to α-crystallin. (A) Fluorescence emission intensity (500 nm) of bis-ANS (10 μM) bound to αA-crystallin (top panel) and αB-crystallin (bottom panel) as a function of bivalent metal ion concentration at 25 °C. The two bivalent metal ions used in this study were Zn^{2+} (empty symbols) and Cu^{2+} (filled symbols). Here the protein concentration was 2.5 μM. The excitation wavelength was 390 nm. (B) Determination of the dissociation constant (K_d) for the interaction between bivalent metal ions and recombinant human αA-crystallin (empty symbols) or αB-crystallin (filled symbols) induced by 1 mM Zn^{2+} (top panel) and 1 mM Cu^{2+} (bottom panel) at 25 °C. The dissociation constant (K_d) was obtained from the slope of the linear plot of $\Delta F/C_{M^{2+}}$ against ΔF, where ΔF represents the increase or decrease in fluorescence intensity (500 nm) at a given concentration of the bivalent metal ion. The dissociation constants (K_d) for the binding of Zn^{2+} to αA- and αB-crystallin are 0.38 ($P < 0.005$) and 0.20 mM ($P < 0.005$), respectively, and those for binding of Cu^{2+} are 0.38 ($P < 0.05$) and 0.26 mM ($P < 0.05$), respectively. The excitation wavelength was 390 nm. The protein concentration was 0.05 mg/mL, and the bis-ANS concentration was 10 μM.

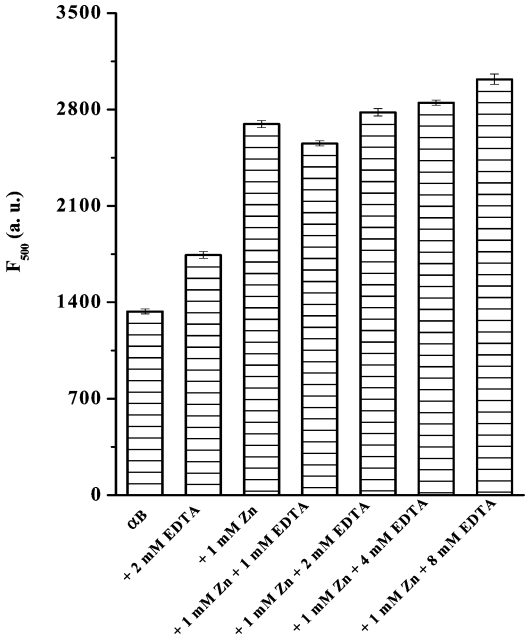

FIGURE 7: Effect of EDTA on the interaction between bis-ANS and αB-crystallin induced by 1 mM Zn^{2+} at 25 °C. The intensities of fluorescence emission of bis-ANS at 500 nm and αB-crystallin were acquired with and without $ZnSO_4$ (1 mM), followed by the addition of EDTA (1−8 mM). The bis-ANS concentration was 10 μM and the αB-crystallin concentration 0.05 mg/mL. The excitation wavelength was 390 nm.

the first 3 min and then reached a steady value in 1 h. This final A_{412} value corresponded to one thiol per subunit of αA-crystallin, in agreement with the previous studies (*55*, *56*). In the presence of 1 mM Ca^{2+}, the kinetic profile was very similar to that without Ca^{2+} ion (trace 2). The presence of 1 mM Cu^{2+} or Zn^{2+} ion in the system somewhat decreased the initial rate of the reaction, but the final A_{412} values were nearly same (traces 3 and 4). This would indicate that Cu^{2+} and Zn^{2+} ions do not have direct bonding with the thiol group, but the conformational changes in αA-crystallin induced by these ions, particularly at the surface level, might have somewhat reduced the initial accessibility of the thiol group to DTNB.

Table 2: Fluorescence Quenching Parameters of Human αB-Crystallin in the Absence and Presence of Various Bivalent Metal Ions at 25 °C

	f_a	K_{SV} (M^{-1})		f_a	K_{SV} (M^{-1})
none	1.0	2.9	1 mM Cu^{2+}	1.0	3.0
1 mM Ca^{2+}	1.0	3.1	1 mM Zn^{2+}	1.0	3.2

Tryptic Digestion of α*-Crystallin in the Presence of Bivalent Metal Ions.* We have checked here whether the addition of selected bivalent metal ions, Zn^{2+}, Ca^{2+}, and Cu^{2+}, changes the digestibility of αB-crystallin by trypsin. At first, we checked if the enzymatic activity of trypsin alone, using BAPNA as a substrate (*46*), was affected by the presence of the bivalent metal ions. We found out that while Zn^{2+} and Ca^{2+} had no effect, 1 mM Cu^{2+} reduced the activity of trypsin by nearly 70%. Further study was carried out with Zn^{2+} and Ca^{2+} only. The SDS−PAGE profile of tryptic digestion products of αB-crystallin in the absence and presence of 1 mM Zn^{2+} at different digestion times using a 1:50 (w/w) ratio of trypsin to chaperone are shown in Figure 10. After digestion for 45 min, it became clear that the presence of Zn^{2+} has considerably slowed the cleavage. After

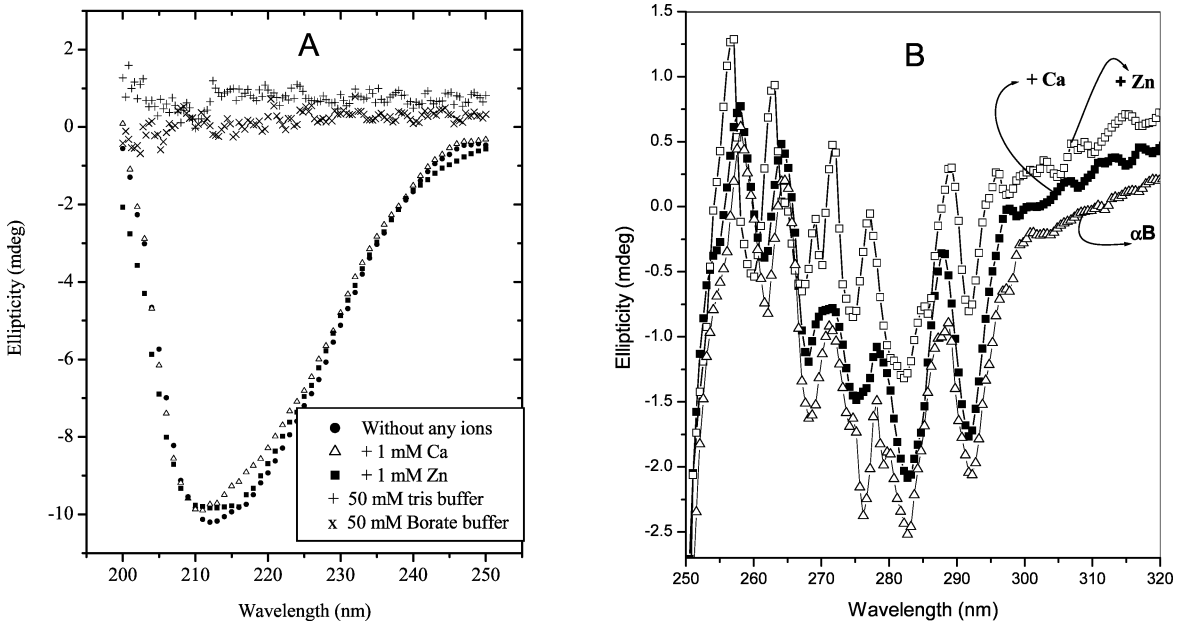

FIGURE 8: Circular dichroic spectra of αB-crystallin in the absence and presence of 1 mM Ca^{2+} and Zn^{2+}: (A) far-UV CD and (B) near-UV CD. The protein concentration in 50.0 mM borate buffer (pH 7.0) of all samples for the far-UV experiment was 0.2 mg/mL, and that for the near-UV experiment was 0.5 mg/mL.

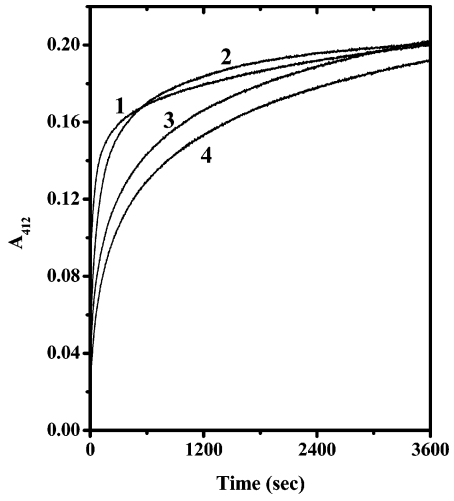

FIGURE 9: DTNB kinetic profiles of αA-crystallin at various concentrations of bivalent metal ions at 25 °C. The αA-crystallin concentration was 0.4 mg/mL, in 50 mM Tris buffer containing 100 mM NaCl (pH 7.4) and DTNB in a 6-fold molar excess over the protein. Absorbance was measured at 412 nm as a function of time: (1) no bivalent metal ions, (2) 1 mM Ca^{2+}, (3) 1 mM Cu^{2+}, and (4) 1 mM Zn^{2+}. All the solutions were incubated for 1 h before the addition of DTNB.

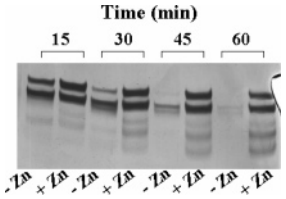

FIGURE 10: SDS−PAGE profile of the trypsin digest of αB-crystallin in the absence and presence of 1 mM bivalent metal ion. αB-Crystallin [1 mg/mL in 50 mM Tris buffer containing 100 mM NaCl (pH 7.0)] was digested with trypsin at a 50:1 (w/w) ratio in the absence and presence of 1 mM Zn^{2+} for different amounts of time at 37 °C.

tryptic digestion for 1.0 h, trypsin completely digested αB-crystallin in the absence of 1 mM Zn^{2+}, but several bands are distinctly visible in the presence of Zn^{2+}, indicating that Zn^{2+} makes αB-crystallin resistant to tryptic digestion. Here also we found that the presence of 1 mM Ca^{2+} had very little influence as the digestion fragment profiles in both the absence and presence of it are practically same (see Figure 1 of the Supporting Information). Use of αA-crystallin in place of αB-crystallin produced no change in the qualitative nature of the result.

Structural Stability of α*-Crystallin in the Presence of Different Bivalent Metal Ions*. We have compared the thermodynamic stability of αB-crystallin by equilibrium urea unfolding in the presence and absence of 1 mM Ca^{2+}, Cu^{2+}, and Zn^{2+} by following tryptophan fluorescence at various urea concentrations. Since the wavelengths of maximum emission (λ_{max}) of native and unfolded αB-crystallin are 337 and 350 nm, respectively, the data were plotted as the ratio of intensities at 337 and 350 nm as a function of urea concentration (Figure 11). All the denaturation profiles of αB-crystallin in the presence and absence of different bivalent metal ions have a sigmoid shape. A crude estimate of the transition midpoint ($C_{1/2}$) from the sigmoidal analysis of the profiles reveals that $C_{1/2}$ remained 2.6 M both in the presence and in the absence of Ca^{2+}. In the presence of 1 mM Cu^{2+}, $C_{1/2}$ marginally increased to 2.9 M. However, 1 mM Zn^{2+} drastically shifted $C_{1/2}$ to >5 M. Even in the presence of 0.1 mM Zn^{2+}, $C_{1/2}$ was 4.6 M urea. The results are indicative of a dramatic increase in the thermodynamic stability of αB-crystallin in the presence of Zn^{2+}.

It can be seen that the profiles lack strong cooperativity, indicating multistate transitions. Sun et al. (*47*) analyzed the unfolding profile of recombinant αB-crystallin with a three-state model according to a native ⇆ intermediate ⇆ unfolded scheme. The profiles presented here in the presence and absence of different bivalent metal ions were also fitted to the three-state model (*10*, *47*, *48*) according to

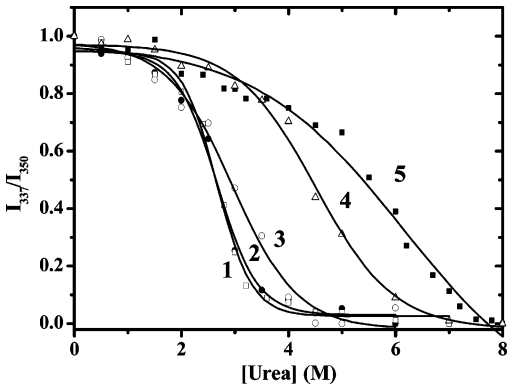

FIGURE 11: Equilibrium urea unfolding profile of αB-crystallin in the absence and presence of different bivalent metal ions at 1 mM and 25 °C: (1) αB-crystallin alone, (2) αB-crystallin and 1 mM Ca^{2+}, (3) αB-crystallin and 1 mM Cu^{2+}, (4) αB-crystallin and 0.1 mM Zn^{2+}, and (5) αB-crystallin and 1 mM Zn^{2+}. The protein concentration was 0.1 mg/mL. The profile has been normalized to a scale of 0−1. Symbols represent the experimental data points, and the solid lines represent the best fit to a three-state model described by eq 3.

$$I = [I_0 + I_1 \exp(-\Delta G_1^\circ + m_1[\text{urea}])/RT + I_\infty \exp(-\Delta G_2^\circ + m_2[\text{urea}])/RT]/[1 + \exp(-\Delta G_1^\circ + m_1[\text{urea}])/RT + \exp(-\Delta G_2^\circ + m_2[\text{urea}])/RT] \quad (3)$$

where I_o, I_1, and I_∞ are the signal intensities for 100% native, 100% intermediate, and 100% unfolded forms, respectively. ΔG_1° refers to the standard free energy change between the native and the intermediate forms, and ΔG_2° refers to the standard free energy change between the intermediate and unfolded forms. ΔG°, being the sum of ΔG_1° and ΔG_2°, refers to the standard free energy change of unfolding (between native and unfolded forms) without urea. The fitted parameters are presented in Table 3. The standard free energy change of unfolding of αB-crystallin at 25 °C in the absence of any bivalent metal ion is 22.6 kJ/mol. This value of ΔG° compares well with that of 21.0 kJ/mol reported by Sun et al. (*47*). Cu^{2+} ion at 1 mM leads to stabilization by approximately 5 kJ/mol, but 1 mM Zn^{2+} increased the ΔG° to 58.7 kJ/mol and thus enhanced its stability ($\Delta\Delta G^\circ$) by ∼36 kJ/mol. That the effect is very specific to Zn^{2+} can be realized from the fact that even at 0.1 mM Zn^{2+} the enhancement of stability is >20 kJ/mol (Table 3). Such a dramatic increase in stability in the presence of Zn^{2+} has also been observed with αA-crystallin and α_L-crystallin (data not shown).

DISCUSSION

The results presented in this paper clearly show that Zn^{2+} ion has a specific interaction with α-crystallin that can result in significant exposure of additional hydrophobic sites on the chaperone surface and consequently can enhance its chaperone activity. We earlier showed that anionic trivalent ATP also produced a qualitatively similar effect (*10*), but compared to that, cationic Zn^{2+} produced a more dramatic effect. The effect is quite specific to Zn^{2+} as many other bivalent ions produced either no effect or a minimal effect. In this regard, it may be mentioned that many early studies (*57*, *58*) that showed aggregation of α-crystallin and cataract formation by Ca^{2+} used much higher concentrations (5−100 mM) of Ca^{2+}. We have restricted ourselves to only 1 mM Ca^{2+}, at which no significant changes in α-crystallin properties have been observed. The key interaction involved in the recognition between chaperone and its substrate is believed to be predominantly hydrophobic in nature. Our results show that Zn^{2+} ions can modulate these hydrophobic interactions of α-crystallin by inducing conformational changes and affecting the global stability of the chaperone. These findings are significant because it shows that such ions may play a crucial role in the structure, function, and stability of the α-crystallin in the lens where there is no protein turnover.

We have shown that the effect of Zn^{2+} is not an ionic strength effect. There seems to be a specific site of interaction of Zn^{2+} on the surface of α-crystallin. The enhancement of bis-ANS fluorescence bound to αB-crystallin (Figure 5B) due to titration by Zn^{2+} indicates binding of Zn^{2+} to the bis-ANS−αB-crystallin complex, and we estimate a dissociation constant (K_d) of 0.2 mM for the Zn^{2+}-bound complex. Interestingly, the dissociation constant (K_d) for the Cu^{2+} was very similar to that of Zn^{2+} ions, but Cu^{2+} ion had a much weaker influence on the functional and structural properties of αB-crystallin. There are a number of negatively charged clusters, such as (Glu^{29},Glu^{33},Asp^{35}), (Asp^{91},Asp^{92},Glu^{95}), and (Glu^{102},Asp^{105},Asp^{106}) in human αA-crystallin and (Glu^{30},-Glu^{34},Asp^{36}), (Asp^{62},Glu^{67},Glu^{71},Asp^{73}), and (Glu^{105},Glu^{106},-Asp^{109},Glu^{110}) in human αB-crystallin (*2*). Formation of a complex between Cu^{2+} and αB-crystallin in which coordination takes place through a mixed donor system consisting of a histidine side chain, carboxylic acid of aspartate and/or glutamate residues, and the nitrogen of the lysine has been proposed (*31*). Recently, Coi et al. (*59*) proposed a molecular model for the most probable coordination site for Zn^{2+} in αB-crystallin where it was shown to be coordinated by the side chains from residues His^{101}, His^{119}, His^{18}, and Glu^{99}. Binding of Zn^{2+} to αB-crystallin resulted in a redistribution of groups at the surface, bringing the donors close enough to coordinate with Zn^{2+} to stabilize its structure. Zn^{2+} ions are so tightly bound to the αB-crystallin that even EDTA was unable to release it.

It is interesting to note here that EDTA itself, being a tetravalent anionic species, can form a complex with α-crystallin, exposing additional hydrophobic pockets very much like ATP (*10*). Since the interaction of EDTA with Zn^{2+}-bound αB-crystallin enhanced hydrophobicity over and above that exposed by Zn^{2+} (Figure 7), it can be safely said that EDTA and Zn^{2+} are interacting with αB-crystallin through different sites.

α-Crystallin has a number of hydrophobic pockets on its surface even at room temperature, as it is known to bind many hydrophobic probes such as ANS, bis-ANS, TNS, pyrene, etc. (*7*, *24*, *52*), but it seems that it also has close to its surface a reserve of extra hydrophobic residues, which can be relocated at the surface by ionic perturbation. Although hydrophobic exposure may occur through partial destabilization of protein structure, stabilization of protein structure by metal binding can change side chain reorientation in proteins (*60*) that can expose further hydrophobic surfaces. If partial unfolding had occurred, it would have caused a substantial loss of tertiary contacts, but this was contrary to what has been reflected in the near-UV spectrum (Figure 8B). We had already seen that perturbation created by ATP led to enhanced exposure of surface hydrophobic pockets to the extent of ∼30%. These results show Zn^{2+} can give rise

Table 3: Parameters of Equilibrium Urea Unfolding of Human αB-Crystallin in the Absence and Presence of Different Bivalent Metal Ions at 25 °C, Obtained from the Three-State Model (N ⇔ I ⇔ U) Fit

system	$\Delta G_1°$ (kJ/mol)	$\Delta G_2°$ (kJ/mol)	$\Delta G°$ (kJ/mol)	m_1 (kJ mol^{-1} M^{-1})	m_2 (kJ mol^{-1} M^{-1})
human αB	6.38 ± 0.38	16.25 ± 0.57	22.63 ± 0.48	5.84 ± 0.45	7.51 ± 0.77
human αB and 1 mM Ca^{2+}	6.34 ± 0.67	16.21 ± 0.72	22.55 ± 0.70	5.75 ± 0.37	8.01 ± 0.50
human αB and 1 mM Cu^{2+}	8.27 ± 0.62	19.49 ± 0.7	27.76 ± 0.68	7.08 ± 0.55	7.61 ± 0.98
human αB and 0.1 mM Zn^{2+}	11.59 ± 0.83	31.67 ± 2.51	43.18 ± 1.67	4.33 ± 0.51	6.97 ± 0.92
human αB and 1 mM Zn^{2+}	16.63 ± 1.17	42.02 ± 3.43	58.65 ± 2.30	7.15 ± 1.13	11.34 ± 1.67

to a more than 100% enhancement in surface hydrophobicity (Table 1 and Figures 4 and 5). A very similar effect of Zn^{2+} was also observed with GroEL; however, in this case, the binding of Zn^{2+} was reversible (*28*), but its effect on the stability of GroEL was not known. The reversible nature of the binding would indicate loose interaction with GroEL, which is also reflected in its K_d being 1 order of magnitude higher than that observed here for α-crystallin. The common features of both these chaperones are the reserve hydrophobicity that can be activated through structural perturbation by small ions. Exposure of additional hydrophobic sites led to enhanced substrate binding (*10*). In this study also, we found that the presence of Zn^{2+} resulted in enhanced substrate binding (data not shown). It is also worth mentioning here that the enhancement of TNS or bis-ANS fluorescence in the presence of Zn^{2+} is not due to an increase in quantum yield as the emission maxima of TNS or bis-ANS remained constant. The enhancement was mostly due to an increase in the extent of probe binding in the presence of Zn^{2+} (Table 1).

It is noted that while Zn^{2+} significantly enhanced the intensity of TNS or bis-ANS fluorescence, some bivalent metal ions such as Cu^{2+}, Ni^{2+}, Fe^{2+}, etc., caused a reduction in fluorescence intensity. Changes in the intensities of bis-ANS fluorescence are usually indicative of the changes in the surface hydrophobicity as they reflect changes in the amount of bis-ANS bound to the protein surface, but since the bis-ANS emission occurs in the visible region (450−550 nm), the colored transition metal ions such as Ni^{2+}, Cu^{2+}, Fe^{2+}, etc., absorb part of this emitted radiation, leading to a quenching of bis-ANS fluorescence. We believe that the intensity reduction for all the colored ions is due to this energy transfer mechanism and not due to a reduction in the exposed hydrophobic surface.

Stability of α-crystallin is a crucial issue, as the human lens does not have much protein turnover (*4*). In vivo, human lens contains 25−250 μg of zinc/g dry weight of the adult lens (*36*, *61*), the physiological role of which is not understood. The concentration of Zn^{2+} (0.1−1 mM) at which the effects are observed is within the repored concentration range of Zn^{2+} in human lens, and hence, the results are physiologically relavant. Our results reveal that Zn^{2+} ions may play a very important role in modulating the stability of α-crystallin (Figure 11). Thus, loss of Zn^{2+} during the aging process may thus lead to a reduction in the chaperone function of α-crystallin. Zinc deficiency has been reported to produce cataract in experimental animals (*37*, *62*−*64*). Zinc supplements are prescribed by doctors for treatment of degenerative eye diseases (*65*); however, experimental results could not establish clear evidence of its beneficial effect (*66*−*69*), and some studies even cautioned against the widespread use of zinc supplements (*70*). We believe our results establish for the first time that zinc is needed for the stabilization of the eye lens protein α-crystallin.

Summarizing, we can say that Zn^{2+} ion plays a vital role in stabilizing the structure and enhancing the chaperone function of α-crystallin. In the absence of protein turnover in the lens, this role of Zn^{2+} may be crucial for the long-term transparency of the lens. Thus, loss of Zn^{2+} because of aging or other causes could be detrimental to the transparency of the eye lens.

ACKNOWLEDGMENT

We thank Dr. W. W. de Jong of The Katholic University and Dr. J. Horwitz of the Jules Stein Eye Institute for the gift of plasmid DNA for αA- and αB-crystallin. We thank Dipak Chandra Konar for his technical assistance during protein purification and CD experiments.

SUPPORTING INFORMATION AVAILABLE

SDS−PAGE profile of trypsin digestion of αB-crystallin in the absence and presence of 1 mM Ca^{2+} (Figure 1). This material is available free of charge via the Internet at http://pubs.acs.org.

REFERENCES

1. Harding, J. J. (1991) *Cataract: Biochemistry, Epidemiology and Pharmacology*, Chapman and Hall, London.
2. Narberhaus, F. (2002) α-Crystallin-type heat shock proteins: Socializing minichaperones in the context of a multichaperone network, *Microbiol. Mol. Biol. Rev. 66*, 64−93.
3. van Montfort, R. L., Basha, E., Friedrich, K. L., Slingsby, C., and Vierling, E. (2001) Crystal structure and assembly of a eukaryotic small heat shock protein, *Nat. Struct. Biol. 8*, 1025−1030.
4. Horwitz, J. (1992) α-Crystallin can function as a molecular chaperone, *Proc. Natl. Acad. Sci. U.S.A. 89*, 10449−10453.
5. Jakob, U., Gaestel, M., Engel, K., and Buchner, J. (1993) Small heat shock proteins are molecular chaperones, *J. Biol. Chem. 268*, 1517−1520.
6. Wang, K., and Spector, A. (1994) The chaperone activity of bovine α-crystallin. Interaction with other lens crystallins in native and denatured states, *J. Biol. Chem. 269*, 13601−13608.
7. Raman, B., and Rao, C. M. (1994) Chaperone-like activity and quaternary structure of α-crystallin, *J. Biol. Chem. 269*, 27264−27268.
8. Farahbakhsh, Z. T., Huang, Q. L., Ding, L. L., Altenbach, C., Steinhoff, H. J., Horwitz, J., and Hubbell, W. L. (1995) Interaction of α-crystallin with spin-labeled peptides, *Biochemistry 34*, 509−516.
9. Das, K. P., and Surewicz, W. K. (1995) Temperature-induced exposure of hydrophobic surfaces and its effect on the chaperone activity of α-crystallin, *FEBS Lett. 369*, 321−325.
10. Biswas, A., and Das, K. P. (2004) Role of ATP on the interaction of α-crystallin with its substrates and its implications for the molecular chaperone function, *J. Biol. Chem. 279*, 42648−42657.
11. Muchowski, P. J., and Clark, J. I. (1998) ATP-enhanced molecular chaperone functions of the small heat shock protein human αB crystallin, *Proc. Natl. Acad. Sci. U.S.A. 95*, 1004−1009.

12. Rawat, U., and Rao, M. (1998) Interactions of chaperone α-crystallin with the molten globule state of xylose reductase. Implications for reconstitution of the active enzyme, *J. Biol. Chem. 273*, 9415−9423.
13. Ganea, E., and Harding, J. J. (2000) α-Crystallin assists the renaturation of glyceraldehyde-3-phosphate dehydrogenase, *Biochem. J. 345* (Part 3), 467−472.
14. Wang, K., and Spector, A. (2001) ATP causes small heat shock proteins to release denatured protein, *Eur. J. Biochem. 268*, 6335−6345.
15. Kim, Y. H., Kapfer, D. M., Boekhorst, J., Lubsen, N. H., Bachinger, H. P., Shearer, T. R., David, L. L., Feix, J. B., and Lampi, K. J. (2002) Deamidation, but not truncation, decreases the urea stability of a lens structural protein, βB1-crystallin, *Biochemistry 41*, 14076−14084.
16. Lampi, K. J., Oxford, J. T., Bachinger, H. P., Shearer, T. R., David, L. L., and Kapfer, D. M. (2001) Deamidation of human βB1 alters the elongated structure of the dimer, *Exp. Eye Res. 72*, 279−288.
17. Koteiche, H. A., and McHaourab, H. S. (2006) Mechanism of a hereditary cataract phenotype. Mutations in αA-crystallin activate substrate binding, *J. Biol. Chem. 281*, 14273−14279.
18. Vicart, P., Caron, A., Guicheney, P., Li, Z., Prevost, M. C., Faure, A., Chateau, D., Chapon, F., Tome, F., Dupret, J. M., Paulin, D., and Fardeau, M. (1998) A missense mutation in the αB-crystallin chaperone gene causes a desmin-related myopathy, *Nat. Genet. 20*, 92−95.
19. Mackay, D. S., Andley, U. P., and Shiels, A. (2003) Cell death triggered by a novel mutation in the αA-crystallin gene underlies autosomal dominant cataract linked to chromosome 21q, *Eur. J. Hum. Genet. 11*, 784−793.
20. Raman, B., Ramakrishna, T., and Rao, C. M. (1995) Temperature dependent chaperone-like activity of α-crystallin, *FEBS Lett. 365*, 133−136.
21. Sharma, K. K., Kaur, H., Kumar, G. S., and Kester, K. (1998) Interaction of 1,1′-bi(4-anilino)naphthalene-5,5′-disulfonic acid with α-crystallin, *J. Biol. Chem. 273*, 8965−8970.
22. Sharma, K. K., Kumar, G. S., Murphy, A. S., and Kester, K. (1998) Identification of 1,1′-bi(4-anilino)naphthalene-5,5′-disulfonic acid binding sequences in α-crystallin, *J. Biol. Chem. 273*, 15474−15478.
23. Saha, S., and Das, K. P. (2004) Relationship between chaperone activity and oligomeric size of recombinant human αA- and αB-crystallin: A tryptic digestion study, *Proteins 57*, 610−617.
24. Kumar, M. S., Kapoor, M., Sinha, S., and Reddy, G. B. (2005) Insights into hydrophobicity and the chaperone-like function of αA- and αB-crystallins: An isothermal titration calorimetric study, *J. Biol. Chem. 280*, 21726−21730.
25. Itzhaki, L. S., Otzen, D. E., and Fersht, A. R. (1995) Nature and consequences of GroEL-protein interactions, *Biochemistry 34*, 14581−14587.
26. Azem, A., Diamant, S., and Goloubinoff, P. (1994) Effect of divalent cations on the molecular structure of the GroEL oligomer, *Biochemistry 33*, 6671−6675.
27. Gorovits, B. M., and Horowitz, P. M. (1995) The chaperonin GroEL is destabilized by binding of ADP, *J. Biol. Chem. 270*, 28551−28556.
28. Brazil, B. T., Ybarra, J., and Horowitz, P. M. (1998) Divalent cations can induce the exposure of GroEL hydrophobic surfaces and strengthen GroEL hydrophobic binding interactions. Novel effects of Zn^{2+} GroEL interactions, *J. Biol. Chem. 273*, 3257−3263.
29. Marini, I., Bucchioni, L., Voltarelli, M., Del Corso, A., and Mura, U. (1995) α-Crystallin-like molecular chaperone against the thermal denaturation of lens aldose reductase: The effect of divalent metal ions, *Biochem. Biophys. Res. Commun. 212*, 413−420.
30. del Valle, L. J., Escribano, C., Perez, J. J., and Garriga, P. (2002) Calcium-induced decrease of the thermal stability and chaperone activity of α-crystallin, *Biochim. Biophys. Acta 1601*, 100−109.
31. Ganadu, M. L., Aru, M., Mura, G. M., Coi, A., Mlynarz, P., and Kozlowski, H. (2004) Effects of divalent metal ions on the αB-crystallin chaperone-like activity: Spectroscopic evidence for a complex between copper(II) and protein, *J. Inorg. Biochem. 98*, 1103−1109.
32. Hawse, J. R., Cumming, J. R., Oppermann, B., Sheets, N. L., Reddy, V. N., and Kantorow, M. (2003) Activation of metallothioneins and α-crystallin/sHSPs in human lens epithelial cells by specific metals and the metal content of aging clear human lenses, *Invest. Ophthalmol. Visual Sci. 44*, 672−679.
33. Okuyama, S., Hashimoto, S., Aihara, H., Willingham, W. M., and Sorenson, J. R. (1987) Copper complexes of non-steroidal antiinflammatory agents: Analgesic activity and possible opioid receptor activation, *Agents Actions 21*, 130−144.
34. Sharma, Y., Rao, C. M., Narasu, M. L., Rao, S. C., Somasundaram, T., Gopalakrishna, A., and Balasubramanian, D. (1989) Calcium ion binding to δ- and to β-crystallins. The presence of the "EF-hand" motif in δ-crystallin that aids in calcium ion binding, *J. Biol. Chem. 264*, 12794−12799.
35. Rajini, B., Shridas, P., Sundari, C. S., Muralidhar, D., Chandani, S., Thomas, F., and Sharma, Y. (2001) Calcium binding properties of γ-crystallin: Calcium ion binds at the Greek key βγ-crystallin fold, *J. Biol. Chem. 276*, 38464−38471.
36. Grahn, B. H., Paterson, P. G., Gottschall-Pass, K. T., and Zhang, Z. (2001) Zinc and the eye, *J. Am. Coll. Nutr. 20*, 106−118.
37. Fabe, J. S., Grahn, B. H., and Paterson, P. G. (2000) Zinc concentration of selected ocular tissues in zinc-deficient rats, *Biol. Trace Elem. Res. 75*, 43−52.
38. Koumantakis, E., Alexiou, D., Grimanis, A., Kaskarelis, D., and Bouzas, A. (1983) Zinc, cobalt and selenium concentrations in the premature and full-term newborn eye, *Ophthalmologica 186*, 41−46.
39. Cardamone, M., and Puri, N. K. (1992) Spectrofluorimetric assessment of the surface hydrophobicity of proteins, *Biochem. J. 282* (Part 2), 589−593.
40. Fersht, A. (1999) *Structure and Mechanism in Protein Science: A Guide to Enzyme Catalysis and Protein Folding*, p 208, Cambridge University Press, New York.
41. Das, K. P., Petrash, J. M., and Surewicz, W. K. (1996) Conformational properties of substrate proteins bound to a molecular chaperone α-crystallin, *J. Biol. Chem. 271*, 10449−10452.
42. Eftink, M. R., and Ghiron, C. A. (1981) Fluorescence quenching studies with proteins, *Anal. Biochem. 114*, 199−227.
43. Provencher, S. W., and Glockner, J. (1981) Estimation of globular protein secondary structure from circular dichroism, *Biochemistry 20*, 33−37.
44. Johnson, W. C. (1999) Analyzing protein circular dichroism spectra for accurate secondary structures, *Proteins 35*, 307−312.
45. Sreerama, N., Venyaminov, S. Y., and Woody, R. W. (1999) Estimation of the number of α-helical and β-strand segments in proteins using circular dichroism spectroscopy, *Protein Sci. 8*, 370−380.
46. Erlanger, B. F., Kokowsky, N., and Cohen, W. (1961) The preparation and properties of two new chromogenic substrates of trypsin, *Arch. Biochem. Biophys. 95*, 271−278.
47. Sun, T. X., Akhtar, N. J., and Liang, J. J. (1999) Thermodynamic stability of human lens recombinant αA- and αB-crystallins, *J. Biol. Chem. 274*, 34067−34071.
48. Das, B. K., Bhattacharyya, T., and Roy, S. (1995) Characterization of a urea induced molten globule intermediate state of glutaminyl-tRNA synthetase from *Escherichia coli*, *Biochemistry 34*, 5242−5247.
49. Bhattacharyya, J., and Das, K. P. (1998) α-Crystallin does not require temperature activation for its chaperone-like activity, *Biochem. Mol. Biol. Int. 46*, 249−258.
50. Lakowicz, J. R. (1983) *Principles of Fluorescence Spectroscopy*, Plenum Press, New York.
51. Das, K. P., Choo-Smith, L. P., Petrash, J. M., and Surewicz, W. K. (1999) Insight into the secondary structure of non-native proteins bound to a molecular chaperone α-crystallin. An isotope-edited infrared spectroscopic study, *J. Biol. Chem. 274*, 33209−33212.
52. Reddy, G. B., Das, K. P., Petrash, J. M., and Surewicz, W. K. (2000) Temperature-dependent chaperone activity and structural properties of human αA- and αB-crystallins, *J. Biol. Chem. 275*, 4565−4570.
53. Biswas, A., and Das, K. P. (2004) SDS induced structural changes in α-crystallin and it's effect on refolding, *Protein J. 23*, 529−538.
54. Augusteyn, R. C., Hum, T. P., Putilin, T. P., and Thomson, J. A. (1987) The location of sulphydryl groups in α-crystallin, *Biochim. Biophys. Acta 915*, 132−139.
55. Spector, A., and Roy, D. (1978) Disulfide-linked high molecular weight protein associated with human cataract, *Proc. Natl. Acad. Sci. U.S.A. 75*, 3244−3248.
56. Bours, J., and Ahrend, M. H. (1990) Staining of free sulfhydryl groups of proteins after separation by isoelectric focusing of Bio-Rad standards and lens crystallins, *Anal. Biochem. 190*, 244−248.

57. Fein, T., Pande, A., and Spector, A. (1979) Further investigation of the role of calcium in human lens protein aggregation, *Invest. Ophthalmol. Visual Sci. 18*, 761−765.
58. Seizen, R., Bindels, J. G., and Hoenders, H. J. (20XX) The quaternary structure of bovine α-crystallin. Effects of variation in alkaline pH, ionic strength, temperature and calcium ion concentration, *Eur. J. Biochem. 111*, 535−444.
59. Coi, A., Bianucci, A. M., Ganadu, M. L., and Mura, G. M. (2005) A modeling study of αB-crystallin in complex with zinc for seeking of correlations between chaperone-like activity and exposure of hydrophobic surfaces, *Int. J. Biol. Macromol. 36*, 208−214.
60. Babor, M., Greenblatt, H. M., Edelman, M., and Sobolev, V. (2005) Flexibility of metal binding sites in proteins on a database scale, *Proteins 59*, 221−230.
61. Sukla, N., Moitra, J. K., and Trivedi, R. C. (1996) Determination of lead, zinc, potassium, calcium, copper and sodium in human catarct lenses, *Sci. Total Environ. 181*, 161−165.
62. Barash, H., Poston, H. A., and Rumsey, G. L. (1982) Differentiation of soluble proteins in cataracts caused by deficiencies of methionine, riboflavin or zinc in diets fed to Atlantic salmon, *Salmo salar*, rainbow trout, *Salmo gairdneri*, and lake trout, *Salvelinus namaycush*, *Cornell Vet. 72*, 361−371.
63. Ketola, H. G. (1979) Influence of dietary zinc on cataracts in rainbow trout (*Salmo gairdneri*), *J. Nutr. 109*, 965−969.
64. Richardson, N. L., Higgs, D. A., Beames, R. M., and McBride, J. R. (1985) Influence of dietary calcium, phosphorus, zinc and sodium phytate level on cataract incidence, growth and histopathology in juvenile chinook salmon (*Oncorhynchus tshawytscha*), *J. Nutr. 115*, 553−567.
65. Newsome, D. A., Swartz, M., Leone, N. C., Elston, R. C., and Miller, E. (1988) Oral zinc in macular degeneration, *Arch. Ophthalmol. 106*, 192−198.
66. Stur, M., Tittl, M., Reitner, A., and Meisinger, V. (1996) Oral zinc and the second eye in age-related macular degeneration, *Invest. Ophthalmol. Visual Sci. 37*, 1225−1235.
67. Mares-Perlman, J. A., Klein, R., Klein, B. E., Greger, J. L., Brady, W. E., Palta, M., and Ritter, L. L. (1996) Association of zinc and antioxidant nutrients with age-related maculopathy, *Arch. Ophthalmol. 114*, 991−997.
68. Smith, W., Mitchell, P., Webb, K., and Leeder, S. R. (1999) Dietary antioxidants and age-related maculopathy: The Blue Mountains Eye Study, *Ophthalmology 106*, 761−767.
69. VandenLangenberg, G. M., Mares-Perlman, J. A., Klein, R., Klein, B. E., Brady, W. E., and Palta, M. (1998) Associations between antioxidant and zinc intake and the 5-year incidence of early age-related maculopathy in the Beaver Dam Eye Study, *Am. J. Epidemiol. 148*, 204−214.
70. Beaumont, P. (1993) Zinc and macular degeneration, *Arch. Ophthalmol. 111*, 1023−1025.

BI7011965